Fermilab

TM-1386
2562.000

TESTS OF A SINGLE-WIRE DRIFT CHAMBER FOR POSSIBLE USE IN LOW INTENSITY BEAMS

H. Haggerty

February 1986

February 18, 1986

Tests of a Single-Wire Drift Chamber for Possible use in Low intensity Beams

H. Haggerty
Facilities Support Department

A single cell drift chamber (active area 4" x 4") with two dimensional readout has been evaluated as a candidate for reliable and inexpensive momentum tagging of low intensity calibration beams. Charges induced on shaped cathode pads allow a measurement of the coordinate parallel to the wire, while the drift time allows a measurement of the position perpendicular to the wire. The design is based on the muon chambers for the D0 detector.[1]

The chamber configuration is shown in figure 1a. Triangular cathode pads are located above, below and to the near side of the wire. On the other side of the wire there are two sets of field shaping electrodes. The conducting surfaces with similar shading are connected together electrically. Both the pads and the field shaping electrodes are etched on .010" G-10 in order to keep the mass in the beam small. The asymmetry of the chamber allows unambiguous track reconstruction in the region between 1" and 5" away from the wire.

Figure 1b shows typical operating voltages of the chamber, and figure 1c shows the cosmic ray test setup used to measure the chamber properties. All three scintillators were 4" by 4".

Two types of amplifiers are used on this device. The pads have low-noise slow amplifiers developed for use in the D0 liquid argon calorimeter[1,2] (fig. 2a). The anode wire uses a simple video amplifier and line driver (fig. 2b). An argon-ethane mix (50/50) was used in all these tests.

The cosmic ray trigger (fig. 3) was kept simple to approximate a possible beam line application.

Two chamber orientations were used during the tests (fig. 4). In configuration A, the chambers were arranged with their wires parallel. In this case the intrinsic resolution of the chambers was measured; the top and bottom cells were used to define a track coordinate and this was compared to the coordinate in the middle chamber. Figure 5a shows the

drift times plotted using this technique. The x axis is the average of drift times in the top and bottom chamber, and the y axis is the drift time in the middle chamber. Splatter seen in these plots is presumably due to delta rays, kinks, and cosmic ray showers. The maximum drift time was about 2.5 microseconds for the 5" maximum drift. The raw time distribution for C2 is shown in figure 5b. Figure 6 shows the projection of figure 5 onto a line perpendicular to a freehand line through the data. The FWHM is .9%, or about 1 mm.

The longitudinal coordinate is obtained by comparing the induced charge on the two sets of pads. Q1 and Q2 denote the magnitude of the induced charges. The normalized charge ratio of chamber "i" is defined as; $R(C_i)=(Q1_i-Q2_i)/(Q1_i+Q2_i)$. Figures 7 shows the charge ratio of the middle chamber versus the average of the charge ratios of the top and bottom chambers. Two cuts were imposed to define a measureable track. First, each chamber was required to have a drift time of less than 3 microseconds. This cut alone reduced the sample by 12%. (This was not due to chamber inefficiency; triggers which had a good drift time in the top and bottom chambers almost always had (>99%) a good drift time in the middle chamber.) The 12% junk rate just reflects the occasional unclean low energy cosmic ray events. The second cut required a charge sample between 25 and 1300 counts on the ADC (4 counts per picoCoulomb) after pedestal subtraction. This cut was more substantial. Here there was a constraint imposed by the dynamic range of the ADC. Figure 8 shows the raw ADC data for events in C2 where there was a good drift time. Although the chambers were operated far from the streamer mode (several hundred Volts), there are occasional large pulses outside the range of the ADC. Without further excuse, the data shown in figure 7 represents 2/3 of the triggers.

Figure 9 shows the charge ratio comparison for those events whose drift times correspond to incidence angles less than about 2 degrees. Not much of an improvement is noted.

Figure 10 shows the effect of one more adjustment of the data. The same events as in figure 9 have had a correction added to compensate for different pad amplifier pulse shapes. That is, since a single ADC gate was generated 3 microseconds after the scintillator trigger, the pad charges

were sampled at different times after their creation, corresponding to the electron drift times in the chambers. (Pulses from tracks near the wire were sampled late on their falling sides; pulses from tracks far from the wire were sampled near their maximum.) Since the amplifiers were not perfect clones, each has slightly different time characteristics. A time dependent correction (a maximum 2% shift) was applied to the data of figure 9 and replotted as figure 10. A slight improvement is seen.

Figure 11 is a projection of the figure 10 data. The FWHM is 2% , or about 2mm. along the wire

Of course, everything that has been presented so far has been a bit of a cheat. There has been no demonstration yet that either of the two coordinate measurements is linear in real space. To make such a measurement the chambers were rearranged from configuration A (figure 4) to configuration B. In this setup, the drift time was plotted against the charge ratio. Previous studies[3,4] indicated that the charge measurements were approximately linear except near the edges of the pads, and that drift times were linear except near the wire. Figure 12 shows drift time (for C1+C3) on the y axis versus R(C2) on the x axis. No cuts have been applied other than requiring a measureable coordinate. There is an apparent loss of resolution for tracks whose avalanches occur near the ends of the anode wire. Figure 12 and 13 show selected events from small angle tracks in different drift time ranges in C2. The difference in these two plots indicate there is some ionization drift parallel to the wire which, if uncorrected, would degrade the resolution in the regions noted.

Rate dependence studies were made by introducing a beta source into chamber C1 and again comparing the center chamber to the average of the top and bottom chamber. The drift time comparison showed no degradation of resolution up to the highest rate from the source (about 20 kHz). For the charge ratio comparison, at 10 kHz a slight deterioration is evident (Figure 15a,Figure 7), while at 20 kHz the signal resolution is worse by a factor of eight (Figure 15b-FWHM=16%, 16mm).

The conclusion drawn from this study is that while the drift time measurement has adequate resolution, the charge ratio measurement is not a viable option for beam line use. The burden imposed by the charge ratio non-linearities, the evident need to calibrate and monitor the charge amplifiers, and the stringent rate limitation in the charge ratio measurement outweigh any advantages of simplicity and economy.

The author would like to acknowledge S. Pordes who suggested building this short version of the D0 muon detector. Much of the electronics was borrowed intact from the early D0 development. Preliminary assembly was done by J. Yamanouchi. Final assembly, quality control and initial testing was done by Jim Welch. Excellent trigger counters were built by W. Burley. Cosmic rays were provided by the luminiferous aether.

References

1. D0 Design Report
2. E740 Proportional Drift Tube Tests, March, 1984 FNAL TM*1301
3. D. F. Anderson et al, CERN-EP/84-01
4. J. Allison et al, Diamond Shaped Cathode Pads for the Longitudinal Coordinate from a Drift Chamber. U. of Manchester, England, preprint

Fig. 1a.

Low Intensity Beam Chamber

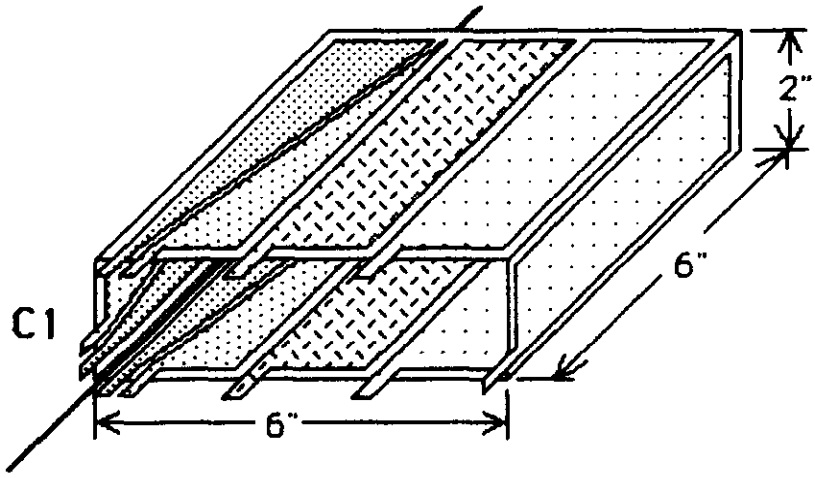

Fig. 1b.

Operating Voltages

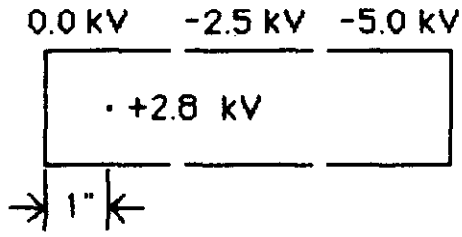

Fig. 1c.

Cosmic Ray Telescope

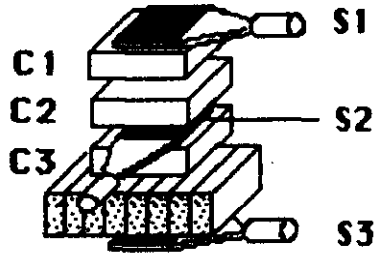

Fig. 2a.

Pad Amplifier

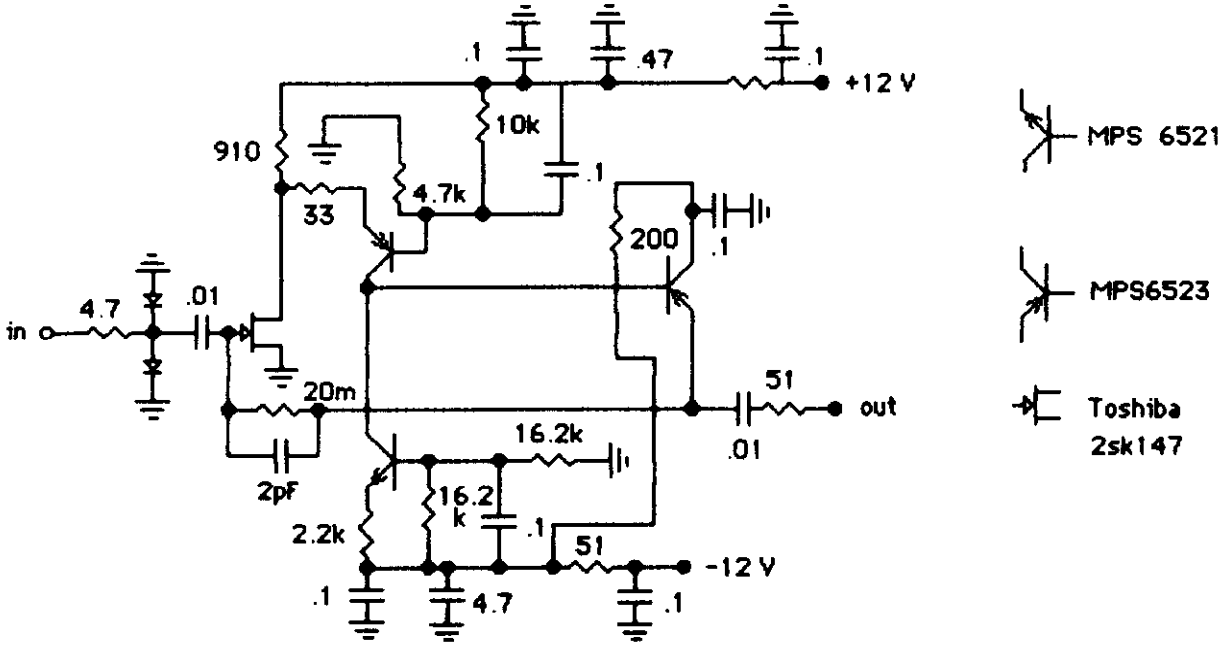

Fig. 2b.

Wire Amplifier

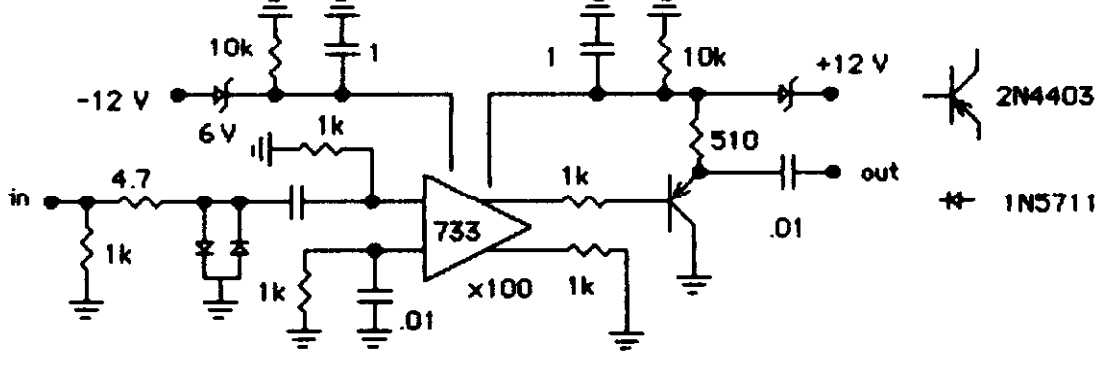

Fig. 3.

Cosmic Ray Trigger

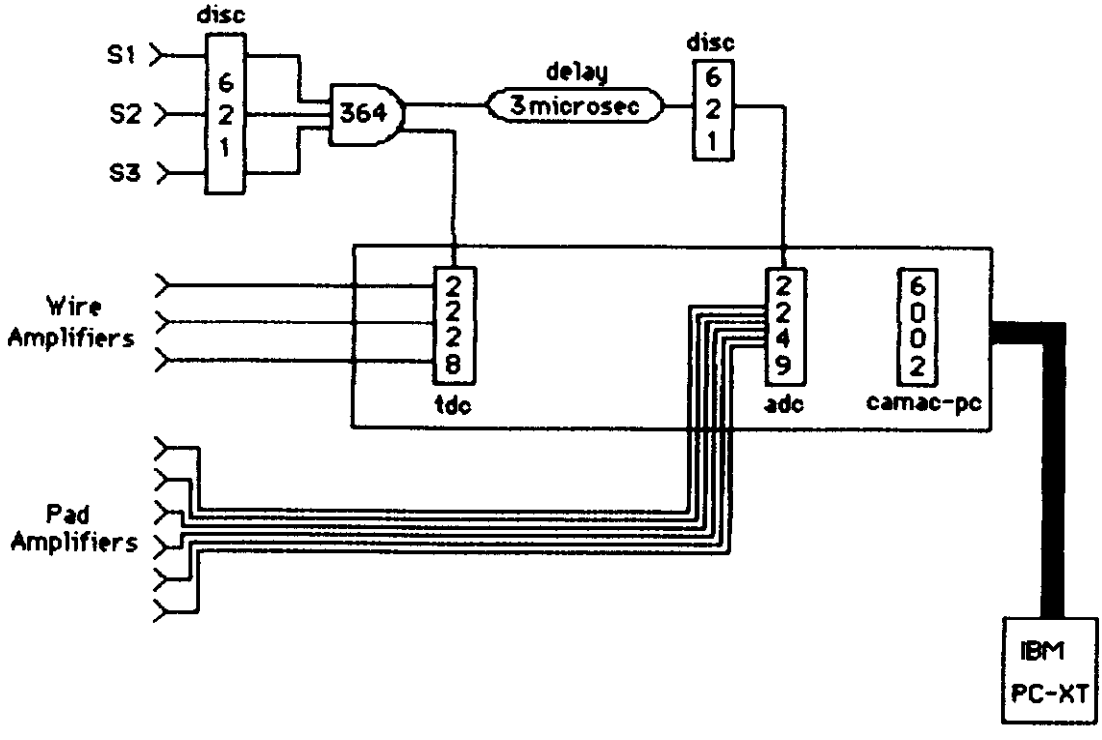

Fig. 4.

Configuration A

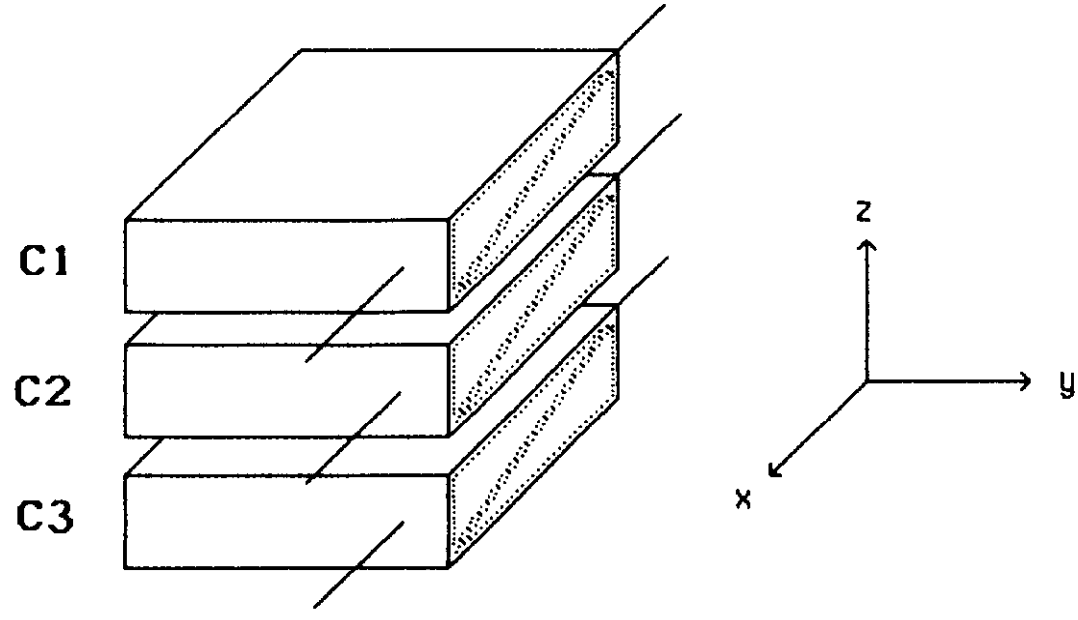

Configuration B

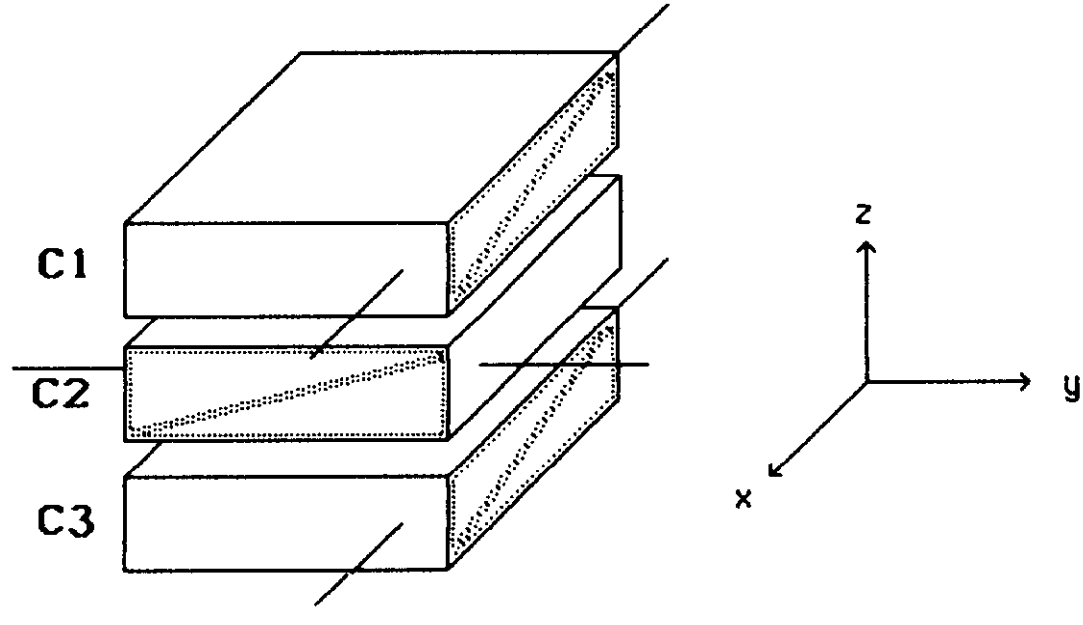

Figure 5a
Drift Time Comparison

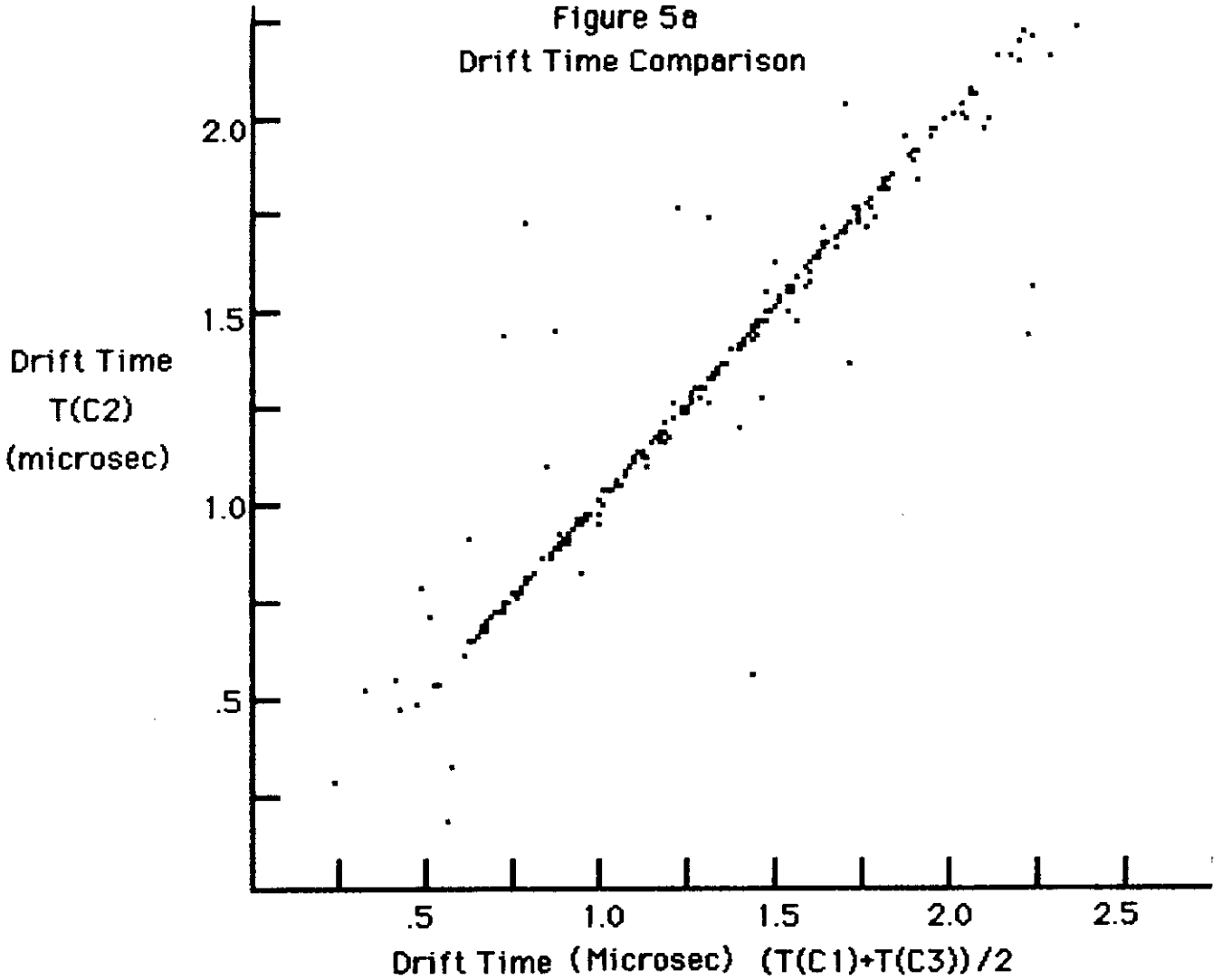

Figure 5b
Raw Time Distribution

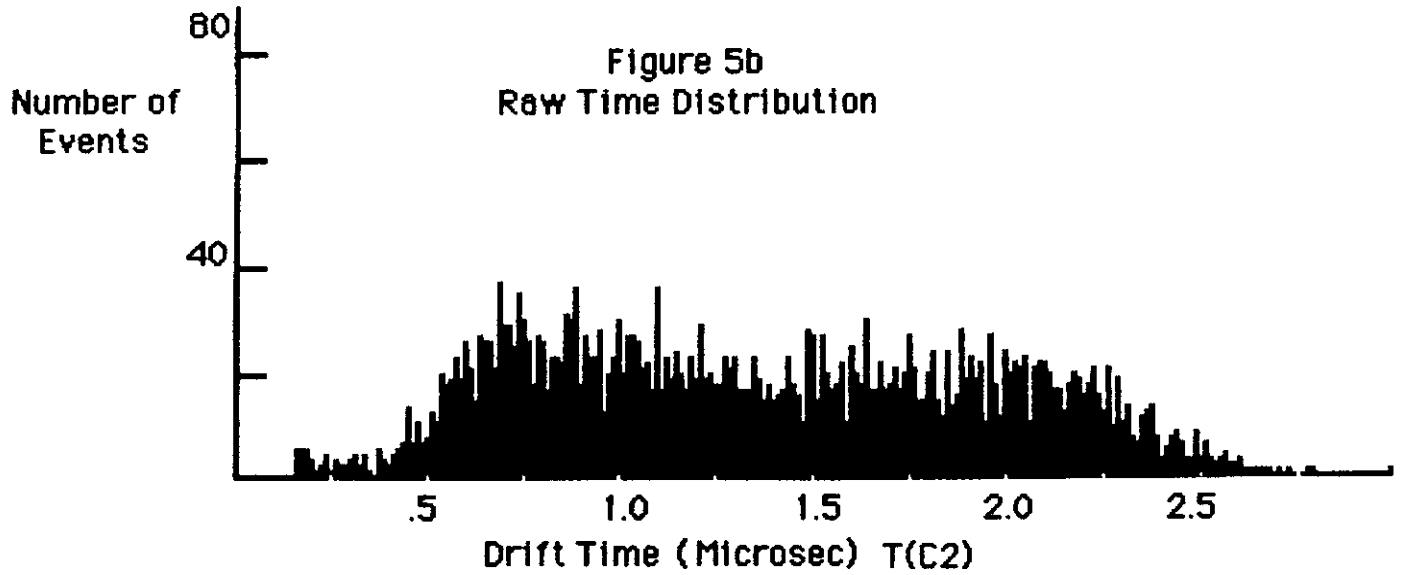

Figure 6
Drift Time Projection

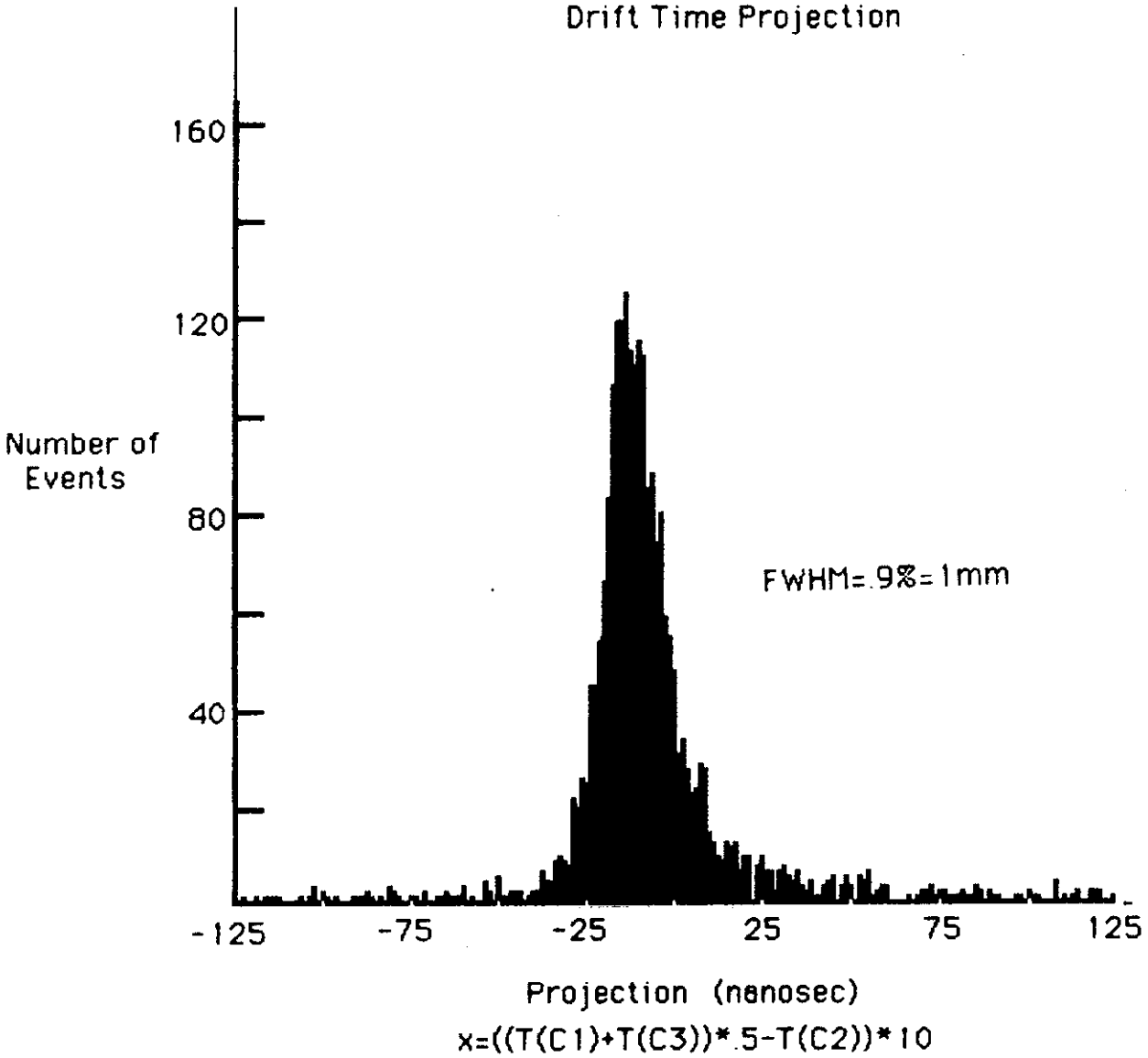

Figure 7.
Charge Ratio Comparison

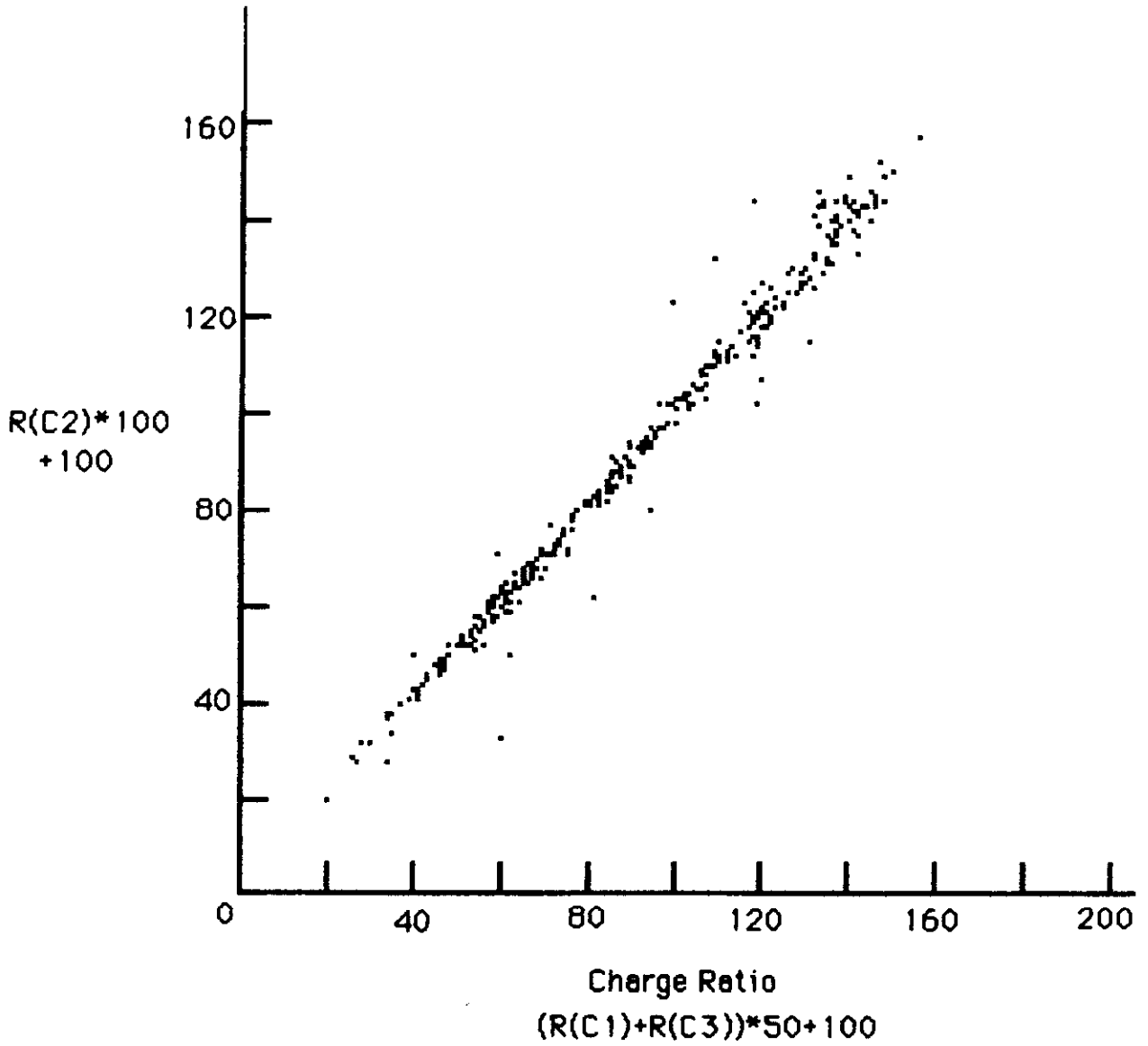

Figure 8
Raw ADC signal

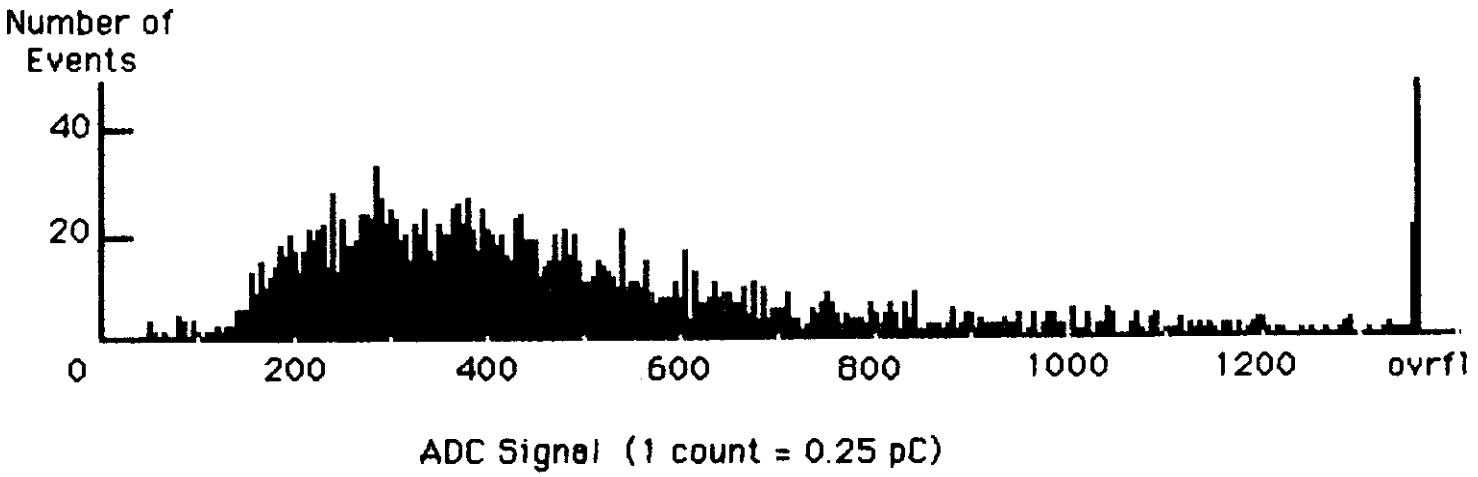

Figure 9.
Charge Ratio Comparison
Vertical tracks

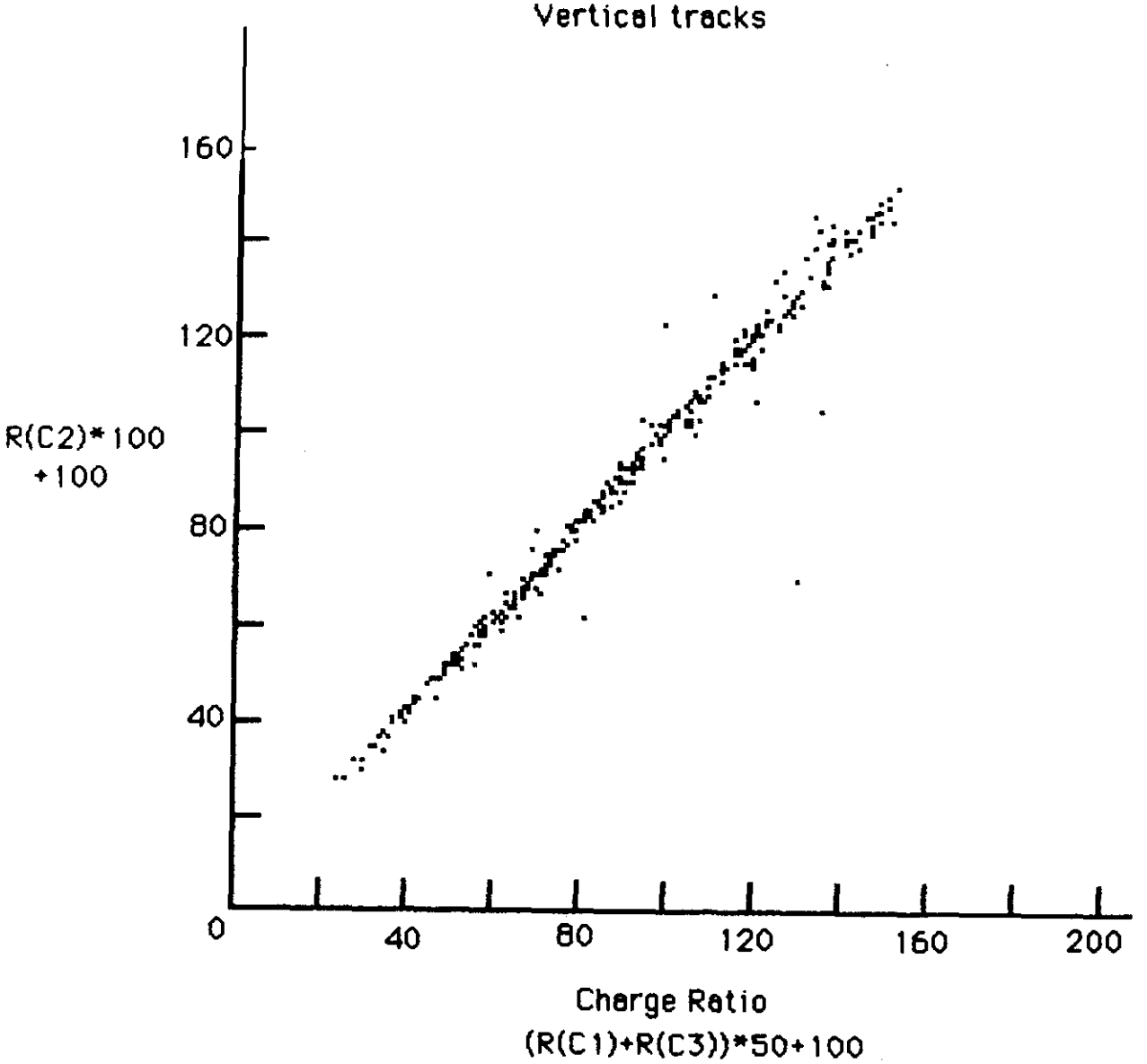

Figure 10.
Charge Ratio Comparison
Vertical tracks + time dependent correction

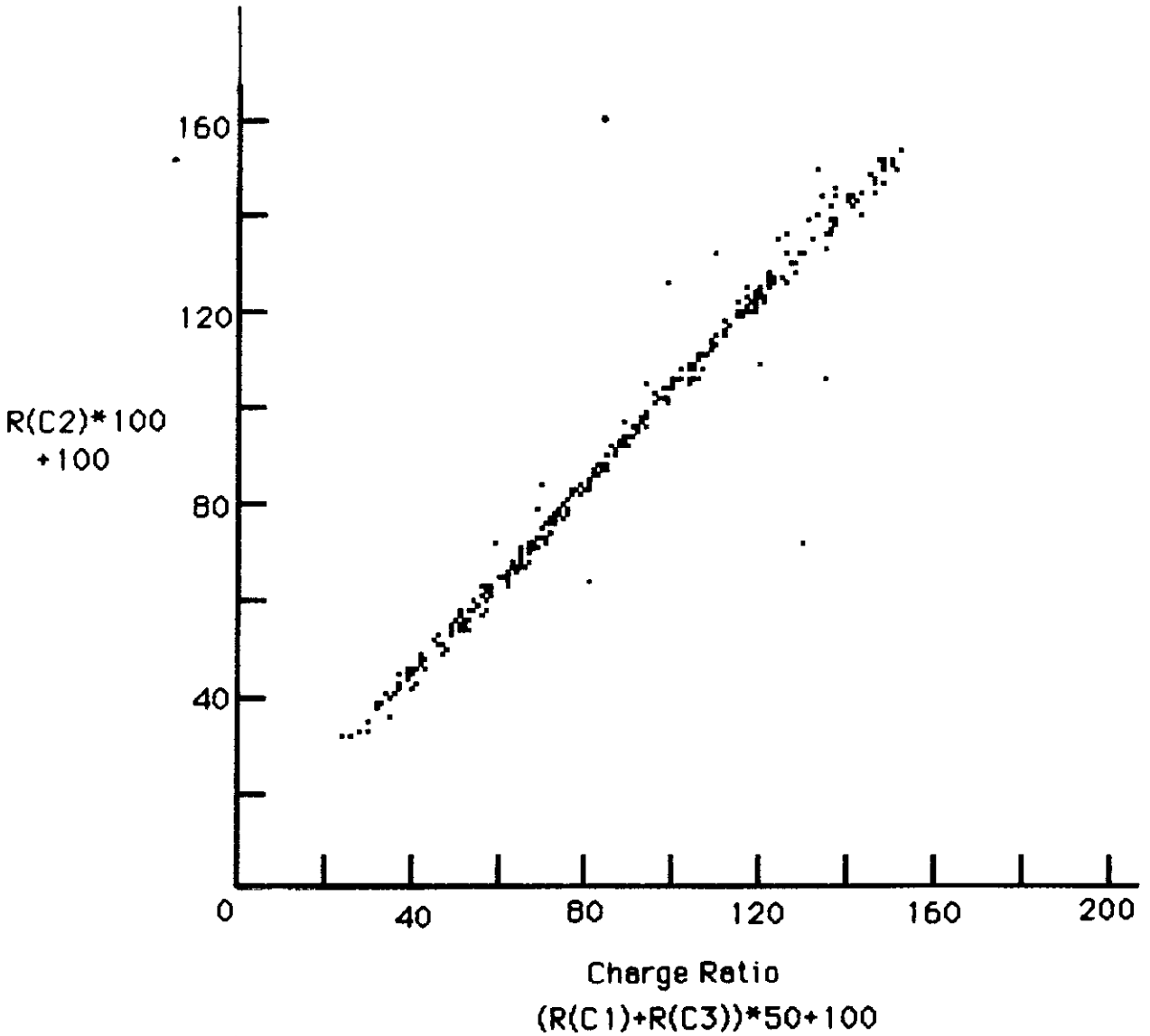

Figure 11
Charge Ratio Projection

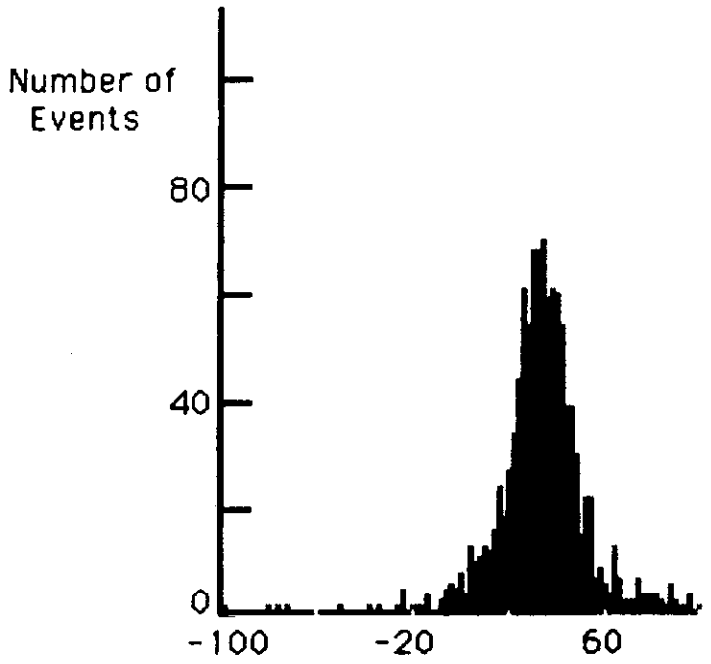

FWHM=2%=2mm

x=(R(C2)+.003*(T(1)+T(3))/100)-(R(C1)+R(C3))*.484)*1000

Figure 12

Time versus charge ratio
Configuration B

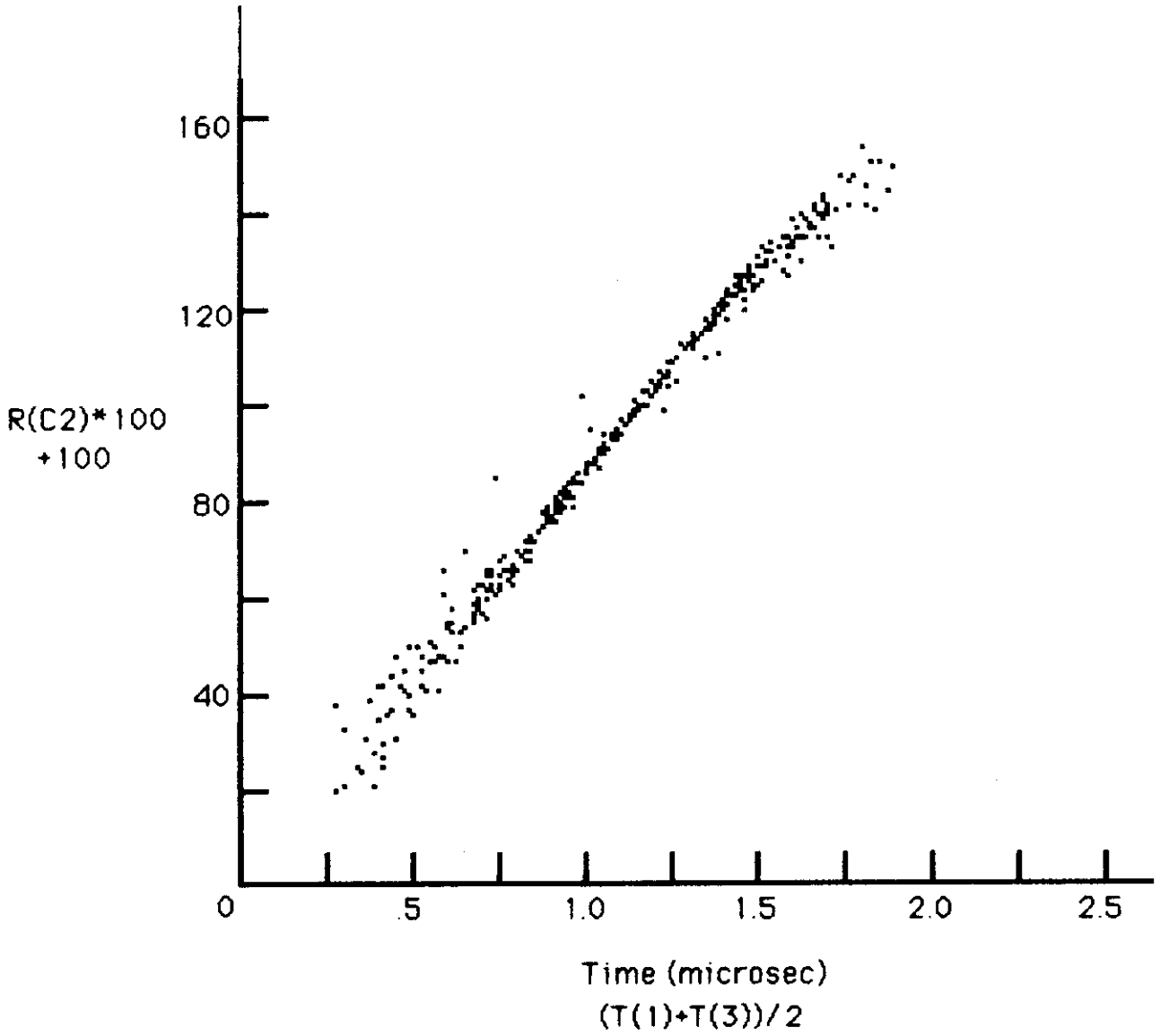

Figure 13

Time versus charge ratio
Configuration B
Long drift in C2

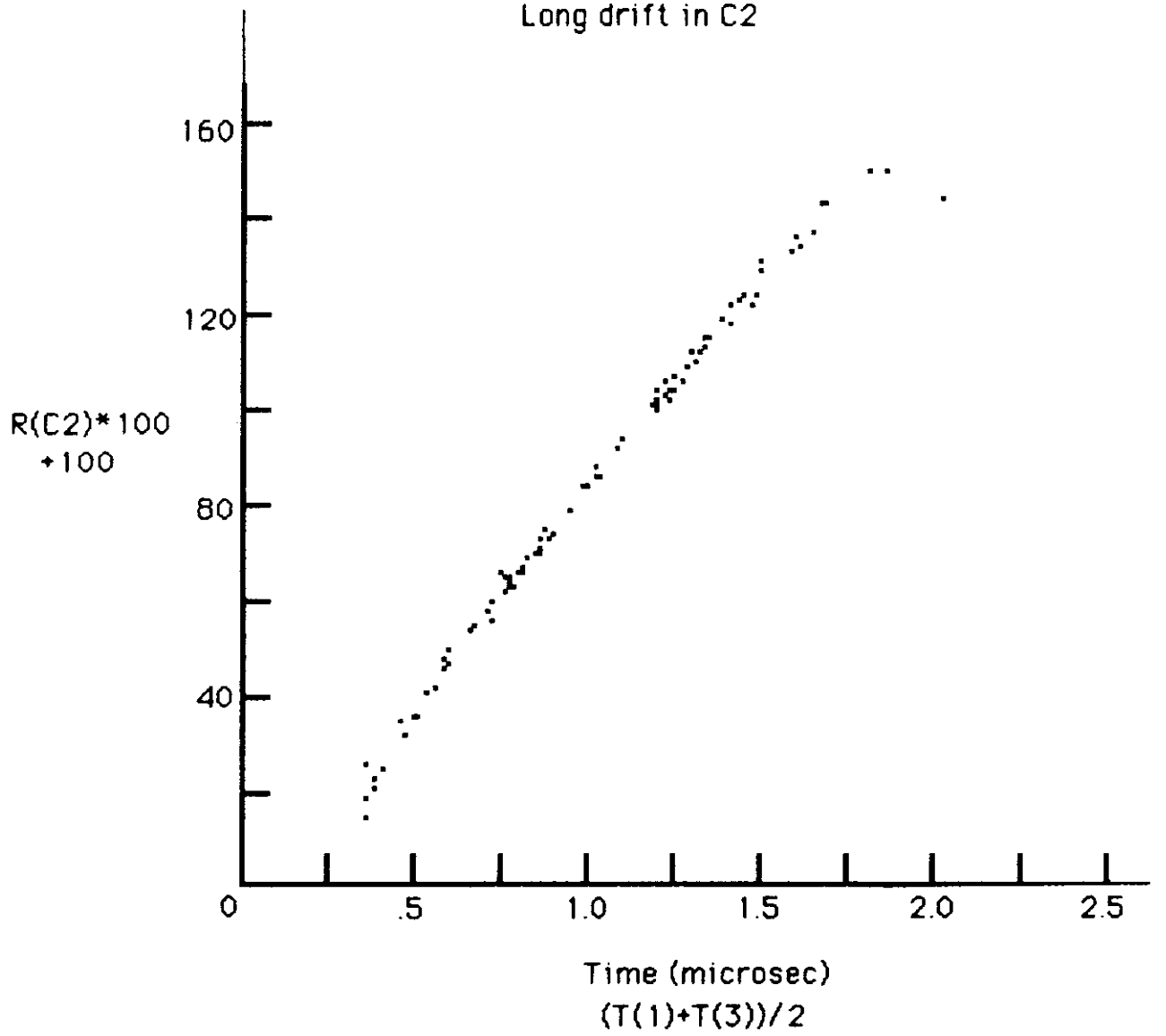

Figure 14

Time versus charge ratio
Configuration B
Short drift in C2

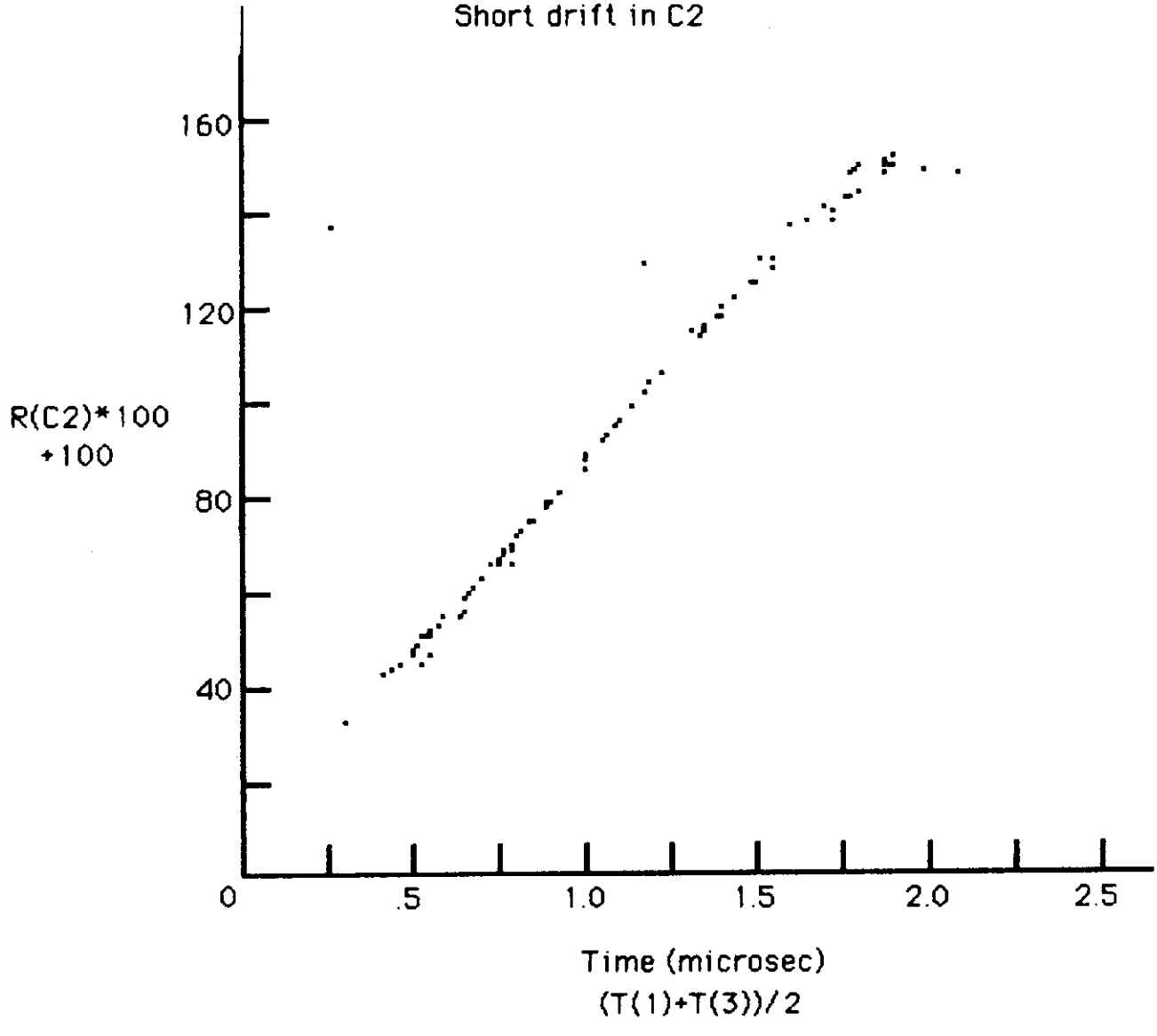

Figure 15a
Charge Ratio Comparison
(with 10 kHz beta source background)

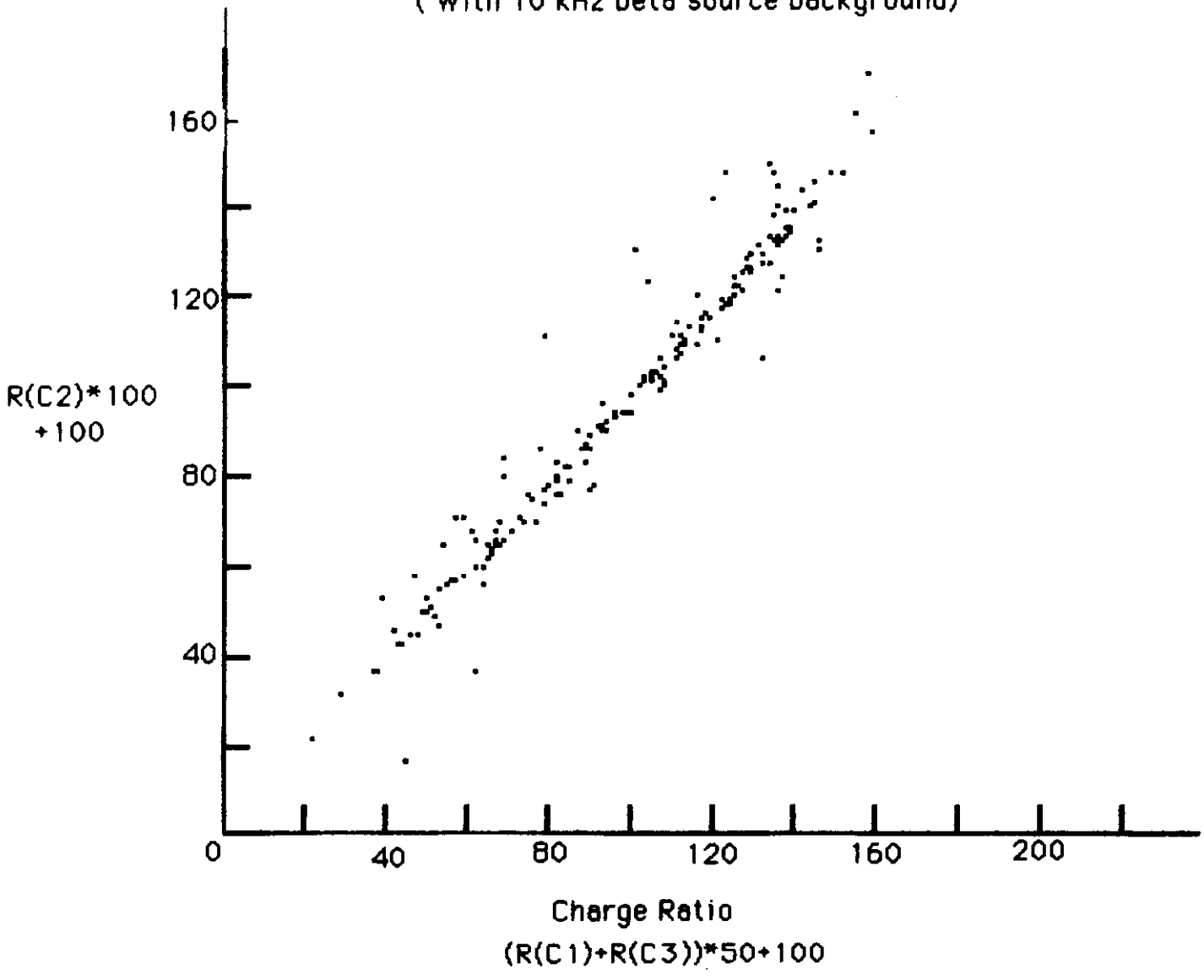
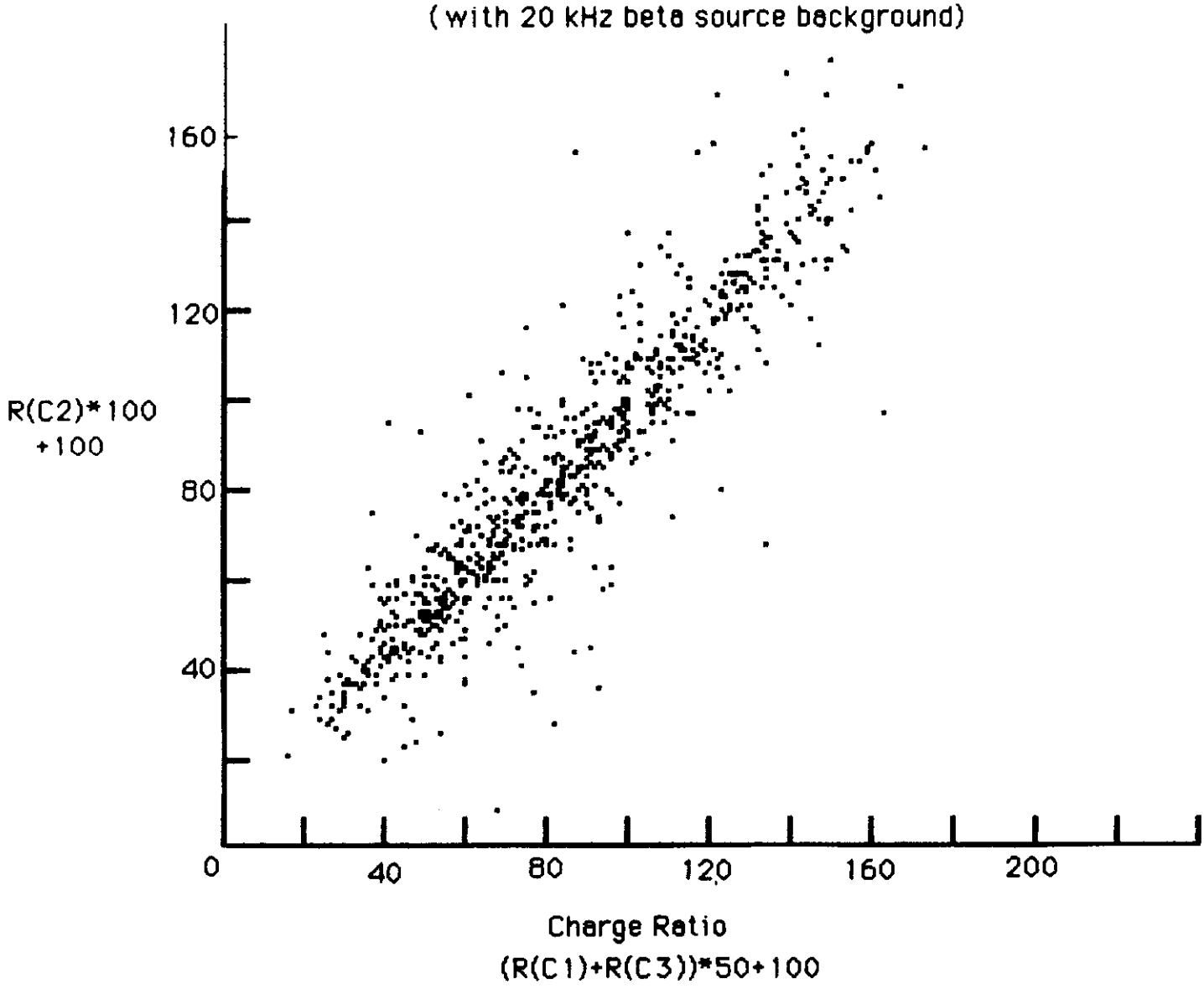
Figure 15b
Charge Ratio Comparison
(with 20 kHz beta source background)